

# Spatial Domain Generation of Random Surface Using Savitzky-Golay Filter for Simulation of Electromagnetic Polarimetric Systems

Shimaa A. M. Soliman<sup>1</sup>, Asmaa E. Farahat<sup>1</sup>, Khalid F. A. Hussein<sup>1</sup>,  
and Abd-El-Hadi A. Ammar<sup>2</sup>

<sup>1</sup>Microwave Engineering Department  
Electronics Research Institute, Cairo, 12622, Egypt  
megahed.shimaa@yahoo.com, asmaa@eri.sci.eg, khalid\_elgabaly@yahoo.com

<sup>2</sup>Electronics and Electrical Communications Department  
Faculty of Engineering, El-Azhar University, Cairo, Egypt  
hady42amar@gmail.com

**Abstract** — A spatial-domain algorithm is introduced for generating both isotropic and anisotropic natural rough surface models with predetermined statistical properties using Savitzky-Golay filter. Unlike the spectral-domain methods, the proposed method does not require the calculation of two-dimensional inverse Fourier transforms which constitute a computational burden for generating large ensembles of high-resolution surfaces. A comparative analysis between the proposed spatial-domain method and one of the conventional spectral-domain methods is presented. The comparison shows that the proposed spatial-domain method results in substantially improved computational performance. The fitness of the generated rough surface to the predetermined statistical properties is verified by calculating a variogram for numerical measurement of the variance and the correlation lengths. To demonstrate the importance of generating such a rough surface for simulation of electromagnetic polarimetric systems, a rough surface with anisotropic statistical properties is placed in the near field region of two antennas of orthogonal polarizations. It is shown that the self and mutual electromagnetic coupling coefficients of the two antennas can be used for measuring the orientation of the rough surface.

**Index Terms** — Polarimetric SAR, rough surface generation, Savitzky-Golay filter.

## I. INTRODUCTION

Many applications make use of electromagnetic (EM) scattering from natural surfaces such as earth remote sensing via imaging synthetic aperture radar (SAR) [1-16]. In such applications it is usually required to numerically generate randomly rough surface (RRS) models with a predetermined set of statistical properties to simulate EM scattering from natural ground surfaces

[17-21]. One often desires to generate a random surface with a particular probability distribution (may be Gaussian with a given mean and variance) and with a specific spatial correlation length. In such simulations it may be an objective to find the relation between the polarization of the backscattered field and the geometrical and electrical properties of the imaged ground surface. The presented work is concerned with the generation of rough surface that is realistic in simulating natural ground surface and to assess the backscattered field due to incident EM waves. The purpose of such a study is to find the relation between the polarization properties of the EM scattering from such surfaces and the geometrical characteristics of the rough surface itself. The main goal is to arrive at numerical results that may be useful for understanding the land images taken by fully polarimetric SAR systems.

The conventional techniques used for generating rough surface models depend on the surface generation in the spectral domain and then the application of the inverse discrete Fourier transformation (IDFT) to get the rough surface heights in the spatial domain [22-24]. However, in some other methods [18], the random surfaces are generated numerically with an arbitrary predetermined distribution function and correlation function of surface roughness. This leads to discretize the surface into a large number of segments, which can be considered uncorrelated roughness (white noise). The resulting profile is then smoothed to get the final model of the rough surface. All these methods arrive at a model for the required random rough surface with good accuracy of the resulting statistical parameters but, however, a great numerical effort is required and the assessment of the agreement with the required statistical properties should be explicitly done in subsequent operations.

The present work introduces a spatial-domain technique for generating anisotropic spatially-correlated random rough surface with predetermined statistical properties (mean height, root-mean-square height and correlation length). This technique applies the Savitzky-Golay filter (SGF) to realize the required correlation lengths between the adjacent heights in two perpendicular directions ( $x$  and  $y$ ). It depends on the generation of a two-dimensional array of uncorrelated Gaussian random numbers that represent surface heights, which are further refined by linear interpolation to get higher resolution of the rough surface points. The SGF is then applied with appropriate smoothing factor and window size to get the surface heights correlated with the desired correlation lengths in both  $x$  and  $y$  directions. Due to the application of SGF the mean value and the variance of the resulting spatially correlated array of random numbers may be different from those predetermined values. For this purpose, the mean value of the resulting array is set to the required value by adding a constant value to the array elements. Also, the array elements are rescaled to get the desired root-mean-squared height.

The method proposed in the present work to generate a random rough surface directly in the spatial domain does not need the heavy mathematical procedures including two-dimensional inverse Fourier transform for high resolution surface models or convolutional integrals required in the other techniques. Moreover, it is simple and capable of generating both isotropic and anisotropic rough surfaces with the predetermined statistical parameters. Furthermore, it insures the fitness of the resulting spatially correlated rough surface to the desired Gaussian distribution and the required statistical properties within a predetermined acceptable error by achieving histogram and variogram measurements.

The present work demonstrates the importance of generating such rough surfaces for EM simulation of the fully polarimetric land imaging synthetic aperture radar systems, and its dependence on the polarization properties of the EM field backscattered from natural rough surfaces.

In the following sections of this paper the statistical properties of the natural rough surfaces, including ergodicity, isotropy and anisotropy, are discussed. The computational procedure of applying the proposed spatial-domain SGF correlation method is described in detail. Also, one of the conventional spectral-domain methods that are commonly used to generate Gaussian rough surface models is described in Appendix A. The numerical results are presented and discussion where a variety of random rough surfaces with various statistical properties are generated. The polarization of the near field backscattered by a rough surface is studied. The dependence of the co-polarized and cross-polarized components of the backscattered field on the geometrical and statistical parameters of the surface is investigated

and discussed. To demonstrate the improved computational performance achieved by the proposed method, a comparative analysis with the conventional spectral-domain technique is presented. The rate of convergence of ensemble averaged coefficients of EM scattering from the generated RSS with the ensemble is investigated and discussed.

## II. STATISTICAL PROPERTIES OF NATURAL RANDOM ROUGH SURFACES

The statistical distribution of the heights of the points on a natural rough surface is most commonly described by a Gaussian probability distribution function with zero mean, which is expressed as:

$$g(z) = \frac{1}{\sigma\sqrt{2\pi}} \exp\left(-\frac{z^2}{2\sigma^2}\right), \quad (1)$$

where  $z$  represents the height of a point on the surface,  $\sigma$  is the standard deviation

The root-mean-squared height,  $h_{rms}$ , of such a rough surface is equal to  $\sigma$  and is often used to give an indication of the “degree of roughness”.

Another important parameter that describes the spatial distribution of the surface heights is the spatial correlation function between adjacent points on the surface. For two points at horizontal locations  $\mathbf{r}$  and  $\hat{\mathbf{r}}$ , respectively, the height-height correlation function is defined as,

$$C_{zz}(\mathbf{r}, \hat{\mathbf{r}}) = \langle z(\mathbf{r})z'(\hat{\mathbf{r}}) \rangle = \int_{-\infty}^{\infty} \int_{-\infty}^{\infty} z z' p(\mathbf{r}, z, \hat{\mathbf{r}}, z') dz dz', \quad (2)$$

where,

$$\mathbf{r} = x \hat{\mathbf{a}}_x + y \hat{\mathbf{a}}_y, \quad (3)$$

where  $x$  and  $y$  are the horizontal coordinates of the point on the rough surface.

### A. Ergodicity, isotropy and anisotropy of the rough surface and the spatial correlation function

In statistics, the term “ergodic” describes a random process for which the global average of one sequence of events is the same as the ensemble average. If the ensemble average is dependent on the ensemble chosen, (i.e. the mean varies from ensemble to ensemble), then the random process is not ergodic. It happens frequently that each realization of the ensemble carries the same statistical information about the homogeneous random process as every other realization. The spatial averages calculated for any realization are then all equal and coincide with the ensemble average. The homogeneous random process is then said to be an ergodic process.

A rough surface is called homogeneous if the characteristics of the surface height distribution over the horizontal dimensions do not change with the horizontal location on the surface. Consequently, the height-height correlation between two points on the surface will depend only on the vector difference,  $\mathbf{r} - \hat{\mathbf{r}}$ , between the horizontal locations,  $\mathbf{r}$  and  $\hat{\mathbf{r}}$ , of the two points. The

rough surface is called isotropic if it has the same characteristics along any direction. For a homogeneous isotropic rough surface, the random process will be "isotropically ergodic" in all the directions. However, some homogenous rough surfaces have their height-height correlation function dependent on the horizontal direction; such a rough surface is "directionally homogeneous" and, consequently, the random process for the surface heights is "directionally ergodic".

For isotropic homogeneous rough surface, the height-height correlation function depends only on the scalar horizontal distance between the two points. For directionally homogenous anisotropic rough surface the height-height correlation function depends on the vector distance between the two points and the expression (2) for the correlation function can be written as:

$$C_{zz}(\mathbf{r}, \mathbf{r}') = C_{zz}(d_x, d_y) = \int_{-\infty}^{\infty} \int_{-\infty}^{\infty} z z' p(z, z', d_x, d_y) dz dz', \quad (4)$$

where,

$$d_x = |x - x'|, \quad d_y = |y - y'|. \quad (5)$$

### B. Two-point height-height probability distribution function

The common types of natural rough surfaces have a Gaussian two-point joint probability distribution function for the heights of any two points on the surface of horizontal separations  $(d_x, d_y)$ .

The correlation length can be qualitatively defined as the maximum length over which two points are correlated. For directionally homogenous anisotropic rough surface, the Gaussian height-height probability density function can be expressed as follows:

$$p(z, z', d_x, d_y) = \frac{1}{2\pi \sqrt{\sigma^4 - C_{zz}^2(d_x, d_y)}} \exp\left(-\frac{\sigma^2(z^2 + z'^2) - 2zz'C_{zz}(d_x, d_y)}{2\sigma^4 - 2C_{zz}^2(d_x, d_y)}\right), \quad (6)$$

where  $C_{zz}(d_x, d_y)$  is the correlation function whose definition is given by (4). The power exponential, or Gaussian, correlation function can be expressed as:

$$C_{zz}(d) = \sigma^2 \exp\left(-\left(\frac{d_x^2}{l_{cx}^2} + \frac{d_y^2}{l_{cy}^2}\right)\right), \quad (7)$$

where  $l_{cx}$  and  $l_{cy}$  are the correlation lengths in the  $x$  and  $y$  directions, respectively.

### III. SPATIAL CORRELATION OF UNCORRELATED RANDOM NUMBERS USING SGF

As the most important and critical process for creating a natural model of rough surface is to correlate the heights of the adjacent points of a two-dimensional array with the required correlation length, this section is

dedicated for the description of the application of SGF [25] on a one-dimension of set of uncorrelated random numbers. The generalization of the method to correlate a two-dimensional set is then described.

The concept of smoothing can be thought of as removing the effect of noise (spatially uncorrelated random values) from a set of measured values. This can simply be achieved by replacing each data point by the average of the surrounding points, because nearby points measure values almost close to each other, so averaging will reduce the effect of the noise.

SGF belongs to the category of digital filters. It is a well-adapted low pass filter used for smoothing data. SGF is used to smooth data in the domain of the data generation, it doesn't require to Fourier transform the data to another domain to remove undesired components and transform back.

For correlating a set of random numbers that represent the values of a random function  $z(x)$  at equally spaced distances along  $x$ -direction, a digital filter is applied to the data values  $z_i \equiv z(x_i)$ , where  $x_i \equiv x_o + i\Delta$  and  $\Delta$  is a constant spacing between points,  $i = \dots - 2, -1, 0, 1, 2, \dots$ . The simplest type of digital filter is the one that replaces each  $z_i$  by a linear combination  $Z_i$  of itself and the neighboring points, that is,

$$Z_i = \sum_{n=-n_L}^{n_R} c_n z_{i+n}, \quad (8)$$

where  $n_L$  is the number of the random values on the left of  $z_i$ , the desired value to be replace, and  $n_R$  is the number of data points to the right of it;  $c_n$  is the weights of averaging. Here it is assumed that we have a moving window of length  $n_L + n_R + 1$  to sequentially scan the values of the vector  $z$ . In each step it replaces the value of the function  $z(x) = z_i$  at the center point of the window by the weighted average of itself and the neighbouring points.

To understand the SGF, let's start by considering the simplest case where all the points have the same weight in equation (8), i.e.,  $c_n = 1 / (n_L + n_R + 1)$ . If the function  $z(x)$  representing these set of points ( $-n_L$  to  $n_R$ ) is constant or is changing linearly with its argument  $x$  (increasing or decreasing), then no bias is introduced in the resulting  $z$  after applying the averaging filter. Under this condition, the moving average technique will preserve the zero-order and the first order harmonic of  $z$ . However, if the function  $z$  has significant second or higher order components, these harmonics will be significantly affected or almost removed by applying a moving average filter. In case these higher order harmonics are of physical interest, then the application of such a moving averaging window filter will result in significant loss of information which may be unacceptable. The idea of SGF is to find coefficients  $c_n$  that preserve higher moments. Equivalently, the idea is to approximate the underlying function within the moving window not by a constant (whose estimate is the

average), but by a polynomial of higher order, typically quadratic, cubic or quartic. For each point  $Z_i$  a polynomial is least-squares fitted to all  $n_L + n_R + 1$  points in the moving window, and then  $Z_i$  is set to be the value of that polynomial at position  $i$ . Simply, the quadratic polynomial will preserve the second order harmonic and the cubic will preserve the third order one and so forth. The smoothing polynomial is found using least square fitting which minimizes the sum of squared differences between an observed value, and the fitted value provided by the filter model.

For a two-dimensional RRS extending in  $x$ - and  $y$ -directions, the height  $z(x, y)$  at each point represents the height function in the  $z$ -direction. The height  $z$  is the function to be smoothed by the SGF. In this case the above procedure is applied on each row of the surface points and then applied on each column consecutively. Applying SGF to the generated Gaussian random heights constituting a rough surface will create a correlation between the heights of the neighbouring points for the surface. The aim is to correlate the surface points with a desired correlation length and preserve the Gaussian probability density function of the surface heights.

#### IV. PROCEDURE OF GENERATION OF SPATIALLY CORRELATED GAUSSIAN ROUGH SURFACE

The main idea behind the method presented here for generating a spatially correlated Gaussian rough surface is to spatially correlate the adjacent elements of two-dimensional array of uncorrelated Gaussian numbers so as to satisfy the required statistical parameters of a natural rough surface as described in Section II. The properties of the resulting array after correlation shall satisfy the following requirements:

- Gaussian distribution of the surface heights,  $g(z)$ ,
- zero mean,  $\mu = 0$ ,
- The standard deviation is equal to the required root-mean-squared height,  $\sigma = h_{rms}$ ,
- The required spatial correlation lengths ( $l_{cx}$  and  $l_{cy}$  in  $x$  and  $y$  directions, respectively),
- The required height-height correlations function,  $C_{zz}(d_x, d_y)$ , and, finally,
- The required two-point joint probability distribution function for the surface heights  $p(z, z', d_x, d_y)$ .

The procedure for the process of generating spatially correlated Gaussian rough surface is described in some detail in the following subsections.

##### A. Generation of two-dimensional uncorrelated Gaussian random data

Two-dimensional arrays of spatially uncorrelated random numbers can be generated to satisfy a set of predetermined statistical parameters such as a specific probability distribution, mean value and variance. Various

generation methods are available in literature [26-28] and can be used to generate such two-dimensional arrays. To generate a realistic model for a natural ground surface, the first step of the procedure is to generate two-dimensional ( $M \times N$ ) array of Gaussian random numbers so as to fit the desired Gaussian probability density function. Let this two-dimensional array of uncorrelated random numbers be  $G(M, N)$ :

$$G(M, N) = \text{GaussianRndGen}(\mu = 0, \sigma = h_{rms}, M, N). \quad (9)$$

##### B. Refinement of the uncorrelated Gaussian random data

To get improved resolution of the uncorrelated random number array and to get it more suitable for subsequent application of the SGF, the generated array is refined by linear interpolation to insert an element between each two successive elements of the random number array. This refinement is carried out in both rows ( $x$ ) and columns ( $y$ ) directions. The dimensions of the refined array for the heights of the rough surface are ( $2M \times 2N$ ). Let the output array of this stage, or the refined version of  $G(M, N)$  be  $G(2M, 2N)$ ; this can be expressed as:

$$G(2M, 2N) = \text{Refine}\{G(M, N)\}. \quad (10)$$

##### C. Application of SGF

For correlating the heights of the adjacent points of  $G$  the SGF, described in Section III, is applied as a smoothing window of length  $W$  points moving sequentially on the array elements to scan the rows and then to scan the columns, thereby correlating all the sequential points lying within the window on both rows and columns. Thus, the SGF acts as a correlator for each group of  $W$  neighbouring array elements. This process can be described by the following equation:

$$G(2M, 2N) = \text{SGF}\{G(2M, 2N, W, W)\}. \quad (11)$$

It is clear that the output of the SGF,  $G(2M, 2N)$ , is a two-dimensional array of correlated random numbers with correlation length of  $W$  points in both the row ( $x$ ) and column ( $y$ ) directions. In this manner, the resulting rough surface has  $(W - 1)$  segments per correlation length in both  $x$  and  $y$  directions. The entire surface has resolution of  $(2M - 1)$  and  $(2N - 1)$  segments along the  $x$  and  $y$  directions, respectively. It is convenient to set  $(2M - 1)$  as well as  $(2N - 1)$  to be integer multiples of  $(W - 1)$ .

If one sets the horizontal separations between the successive surface rows and columns to  $\Delta x$  and  $\Delta y$ , respectively, the resulting correlation lengths will be  $l_{cx} = (W - 1)\Delta x$  and  $l_{cy} = (W - 1)\Delta y$ . It should be noted that  $\Delta x$  and  $\Delta y$  can be arbitrarily set to get the predetermined values of  $l_{cx}$  and  $l_{cy}$ . In this way, the

width and length of the entire rough surface are  $L_x = (2M - 1)\Delta x$  and  $L_y = (2N - 1)\Delta y$ .

For accurate results of EM scattering, the number of segments per correlation length should be large enough, i.e.,  $W - 1 \gg 1$ . In the same time, the electrical length of one segment should be small enough, i.e.,  $\Delta x \ll \lambda$  and  $\Delta y \ll \lambda$ , where  $\lambda$  is the free space wavelength.

#### D. Preserving the required mean and standard deviation of resultant rough surface

Due to the refinement and the application of SGF processes to the uncorrelated two-dimensional Gaussian numbers as described in Sections IV.B and IV.C, both the mean value and the standard deviation of the resulting may become different from the target values required for the final heights of the rough surface.

Let the mean value and the variance of  $G$  be:

$$\mu_S = \text{Mean}(G), \quad (12)$$

$$\sigma_S^2 = \text{Variance}(G). \quad (13)$$

To preserve zero mean of the finally generated rough surface, the mean value  $\mu_S$  is subtracted from each element of the array  $G$ . The resulting array is then scaled by a factor  $h_{rms}/\sigma_S$  to get the final value of the standard deviation equal to the target value,  $h_{rms}$ . This process can be described as follows:

$$z(2M, 2N) = \frac{h_{rms}}{\sigma_S} (G - \mu_S). \quad (14)$$

#### E. Variogram for measuring the statistical properties of the final rough surface

To check the fitness of the resulting spatially correlated rough surface to the predetermined statistical properties, a variogram is calculated for numerical measurement of the variance  $h_{rms}^2$  and the correlation lengths  $l_{cx}$  and  $l_{cy}$  in  $x$  and  $y$  directions, respectively. The variogram is an indication of how the spatial data are related with distance, therefore it's a measure of the correlation length  $l_c$  in a specific direction. The variogram for lag vector  $\mathbf{h}$  is defined as the average squared difference of values separated approximately by  $\mathbf{h}$  and is expressed as follows:

$$\gamma(\mathbf{h}) = \frac{1}{N(\mathbf{h})} \sum_{\alpha=1}^{N(\mathbf{h})} [z(\mathbf{r}_\alpha + \mathbf{h}) - z(\mathbf{r}_\alpha)]^2, \quad (15)$$

where,  $\mathbf{h} = h_x \hat{\mathbf{a}}_x + h_y \hat{\mathbf{a}}_y$  is the lag vector representing the vector separation between two spatial locations,  $\mathbf{r} = x \hat{\mathbf{a}}_x + y \hat{\mathbf{a}}_y$  is the horizontal vector of spatial coordinates,  $z(\mathbf{r}_\alpha)$  is the (height) variable under consideration as a function of the spatial location  $\mathbf{r}_\alpha$ ,  $z(\mathbf{r}_\alpha + \mathbf{h})$  is lagged version of variable under consideration,  $N(\mathbf{h})$  is the count of all pairs of points having vector separation  $\mathbf{h}$ .

Figure 1 shows a model plot of the variogram against the lag distance  $h$ . After a long enough lag

distance the plotted curve becomes constant and equal to the variance and the random data are no more correlated. The correlation length  $l_c$  (in the direction of  $\mathbf{h}$ ) is the lag distance at which the variogram reaches about 63% of the variance whereas the range ( $3l_c$ ) is the lag distance at which the variogram reaches about 95% of the variance.

By setting  $\mathbf{h} = h_x \hat{\mathbf{a}}_x$ , the variogram can be plotted and fitted to the following exponential function from which one can deduce the correlation length in the  $x$  direction:

$$\gamma(h_x) = h_{rms}^2 (1 - e^{-h_x/l_{cx}}). \quad (16)$$

Similarly, by setting  $\mathbf{h} = h_y \hat{\mathbf{a}}_y$ , the variogram can be plotted and fitted to the following exponential function from which one can deduce the correlation length in the  $y$  direction:

$$\gamma(h_y) = h_{rms}^2 (1 - e^{-h_y/l_{cy}}). \quad (17)$$

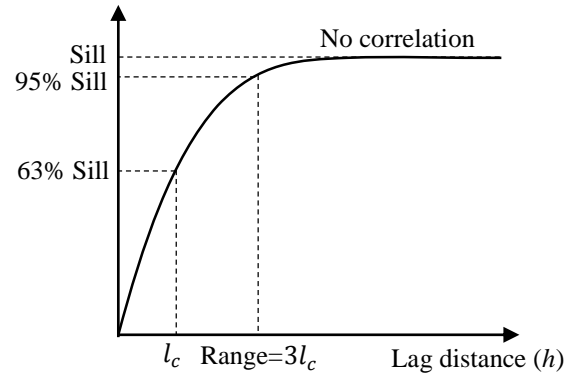


Fig. 1. Variogram of the rough surface model.

## V. POLARIZATION CHARACTERISTICS OF THE SCATTERED NEAR FIELD

To demonstrate the importance of generating a random rough surface for the simulation of electromagnetic polarimetric systems, an anisotropic rough surface with predetermined statistical properties is placed in the near field region of two coplanar linearly polarized antennas of orthogonal polarizations.

The antenna arrangement is shown in Fig. 2. To account for the vertical and horizontal polarizations of the backscattered field, two orthogonal dipoles (crossed dipoles) are used as transmitter/receiver. One of the two dipoles is vertically oriented whereas the other one is horizontally oriented.

The crossed dipole antennas are designed to get a perfect impedance matching for negligible reflection coefficient. The generated rough surface has a perfectly electric conducting material. It is shown that the self and mutual electromagnetic coupling coefficients of the two antennas can be used for measuring the orientation of the rough surface.

Let  $E_{vt}$  and  $E_{vr}$  be the transmitted and received

electric fields, respectively, at the port of the vertical dipole and let  $E_{ht}$  and  $E_{hr}$  be the transmitted and received electric fields, respectively, at the port of the horizontal dipole.

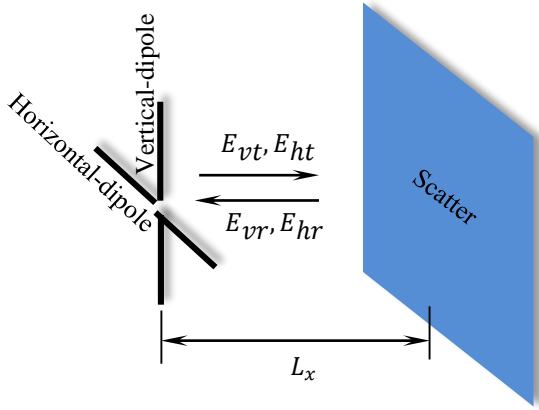


Fig. 2. The configuration of the antenna system used to study the polarization characteristics of the near field scattered from the rough surface.

The edges bounding the rough surface due to the geometrical truncation are not found in the real (natural) surfaces. For an incident plane wave the entire rough surface including its truncation edges will be illuminated; in this case, the edges would significantly contribute to the EM scattering. Therefore, a Gaussian beam may be a solution to avoid the surface edge contribution. However, in the present work another solution is employed to avoid such unwanted effect. The dipoles used to calculate the (near zone) scattering parameters are very short relative to the rough surface dimensions. Moreover, they are placed near the center of the truncated rough surface (i.e., far from the edges) which causes the interaction between the dipoles and the rough surface edges to be very weak and of insignificant contribution to the scattering parameters calculated at the antenna ports.

Let the port of the vertical dipole be denoted as (1) and the horizontal one as (2). To calculate the co-polarized component of the field backscattered from the arbitrary surface we consider the following parameters,

$$S_{vv} \equiv S_{11} = \left. \frac{E_{vr(1)}}{E_{vt}} \right|_{E_{ht}=0}, \quad (18)$$

where  $E_{vr(1)}$  is the electric field received by the vertical dipole when the same dipole is acting as a transmitter:

$$S_{hh} \equiv S_{22} = \left. \frac{E_{hr(2)}}{E_{ht}} \right|_{E_{vt}=0}, \quad (19)$$

where  $E_{hr(2)}$  is the electric field received by the horizontal dipole when the same dipole is acting as a transmitter. Also, to calculate the cross-polarized component of the backscattered field we consider the following parameters:

$$S_{hv} \equiv S_{21} = \left. \frac{E_{hr(1)}}{E_{vt}} \right|_{E_{ht}=0}, \quad (20)$$

where  $E_{hr(1)}$  is the electric field received by the horizontal dipole when the vertical dipole is acting as a transmitter.

$$S_{vh} \equiv S_{12} = \left. \frac{E_{vr(2)}}{E_{ht}} \right|_{E_{vt}=0}, \quad (21)$$

where  $E_{vr(2)}$  is the electric field received by the vertical dipole when the horizontal dipole is acting as a transmitter.

## VI. RESULTS AND DISCUSSION

The presentation of the numerical results in this section aim to investigate the theoretical and procedural issues discussed in the previous sections. The capability of the algorithm developed for applying SGF to generate a random rough surface which maintains the target statistical parameters as required is numerically investigated. The numerical results concerned with the generation of a variety of both isotropic and anisotropic rough surfaces with various statistical parameters such the correlation lengths in  $x$  and  $y$  directions are presented. Other results are presented to verify that the generated rough surface realizes the target statistical parameters such as the overall Gaussian distribution of the surface heights, the correlation lengths in the different directions, the root-mean-squared height, the two-point height-height joint probability density function and the correlation function. Finally, the numerical results concerned with the polarization properties of the scattered field from rough surface are demonstrated for the purpose of relating the properties of the backscattered field to the statistical properties of the RRS itself.

### A. Application of SGF to spatially correlate two-dimensional random data

As described in Section 4.1, the first step of generating a spatially correlated random rough surface with the desired statistical properties is to generate a  $M \times N$  array of uncorrelated Gaussian random numbers with zero mean and unity variance. These random numbers can be considered as the heights of a spatially uncorrelated rough surface. The Matlab “normrnd()” function is used to generate  $100 \times 100$  array of uncorrelated random numbers. A three-dimensional plot of such an array with  $M = N = 100$  is shown in Fig. 3. These random numbers are 10,000 data samples of spatially uncorrelated heights, which are to be subjected to the procedure described in Section IV.C to generate the spatially correlated rough surface with the desired statistical properties.

As described in Section IV.B, the resolution of the uncorrelated two-dimensional array presented in Fig. 3 is doubled by inserting an extra point between each two successive points of the original array by linear

interpolation to obtain a two-dimensional array of  $200 \times 200$  elements. To get a spatially correlated rough surface of size  $200 \times 200$  points with 18 points correlation length, the SGF with a smoothing window of 18-point length is applied to correlate the random numbers on each row and column as described in Section IV.C.

Figure 4 shows the resulting spatially correlated Gaussian random rough surface with  $\mu = 0$ ,  $h_{rms} = 1.0$ , and  $l_{cx} = l_{cy} = 18$  points. Figure 5 presents a comparison between the spatially correlated rough surface (after the application of SGF correlation method) and the uncorrelated random numbers for 100 points lying on the central row of the two-dimensional array.

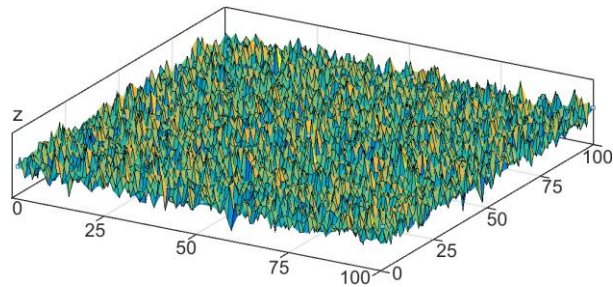


Fig. 3. Plot of two-dimensional array of  $100 \times 100$  uncorrelated Gaussian random numbers with zero mean and unity standard deviation.

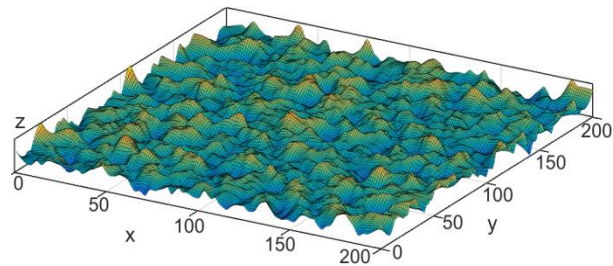


Fig. 4. Plot of the spatially correlated rough surface generated by applying the procedure described in Section IV to the uncorrelated Gaussian array presented in Fig. 3.

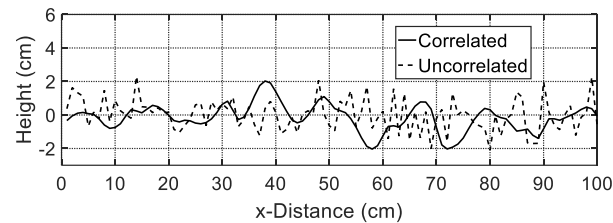


Fig. 5. Comparison between the spatially correlated rough surface and the uncorrelated random numbers for 100 points lying on the central row of the two-dimensional array.

The correlation length can be numerically measured using the variogram as described in Section IV.E. The measured variogram of the generated RRS is plotted as shown in Fig. 6. The fitted curve for the variogram gives a correlation length of 18 points, which is exactly as desired. This indicates the accuracy and efficiency of the proposed method for generating a rough surface with predetermined statistical properties.

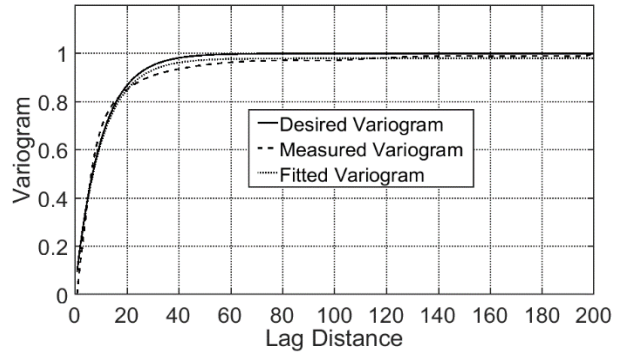


Fig. 6. Variogram of the spatially correlated rough surface generated by the SGF correlation method.

**B. Comparative analysis between the spectral and spatial domain techniques of rough surface generation**

Numerical comparisons between the proposed spatial-domain method and the conventional spectral-domain methods of generating RRS are presented. The following comparisons are concerned with accuracy of the statistical parameters of the generated RRS and some computational performance metrics such as the computational time and memory space requirements.

**B.1 Fitness of the generated rough surface to the predetermined statistical model**

One-dimensional 100-point resolution rough surfaces generated by the proposed spatial-domain method and the conventional spectral-domain method are presented in Fig. 7 (a) and Fig. 7 (b), respectively.

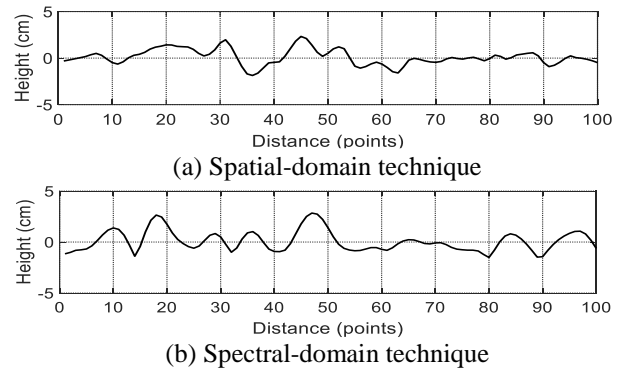


Fig. 7. One-dimensional rough surfaces generated by the spatial-domain and the spectral-domain methods.

Three-dimensional plots of  $20 \times 20$  cm rough surfaces generated using both the spatial and spectral domain techniques are presented in Fig. 8 (a) and Fig. 8 (b), respectively. Both surfaces are isotropic with  $l_{cx} = l_{cy} = 2$  cm. Figure 9 presents anisotropic rough surfaces generated using both techniques with  $l_{cx} = 0.2l_{cy} = 2$  cm. The corresponding variograms of the two rough surfaces are plotted in Fig. 10. Comparing the variograms of the two surfaces shows that both the spatial-domain and spectral-domain methods are successful in generating rough surfaces that accurately satisfy the predetermined statistical properties.

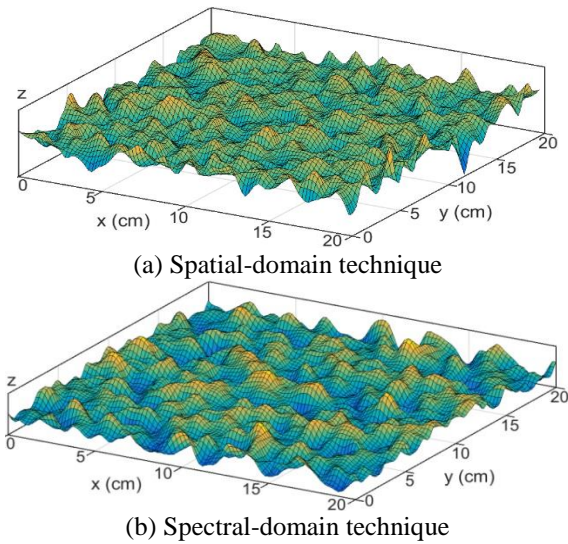


Fig. 8. Rough surfaces of dimensions  $20 \times 20$  cm generated using the spatial and spectral methods,  $l_{cx} = l_{cy} = 2$  cm.

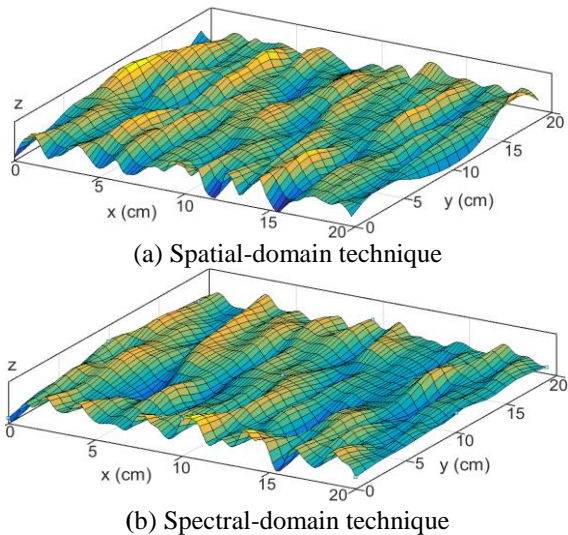


Fig. 9. Rough surfaces of dimensions  $20 \times 20$  cm generated using the spatial and spectral methods,  $l_{cx} = 0.2l_{cy} = 2$  cm

**B.2. Computational performance**

To generate a surface of  $N \times N$  discrete points using the spectral domain method described in Appendix A, one has to compute a two-dimensional  $(N \times N)$  IDFT. For large values of  $N$ , this takes a substantially larger computational time than that taken by the proposed spatial-domain method to generate the same surface.

For the sake of comparing the computational performance of the proposed spatial domain technique to that of the conventional spectral domain one, a  $10 \times 10$  cm rough surface with statistical parameters:  $l_{cx} = l_{cy} = 1$  cm,  $\sigma = 1$  cm and  $\mu = 0$ , has been generated using both of them. The surface dimensions are  $N \times N$  points; a higher value of  $N$  produces a surface of higher resolution.

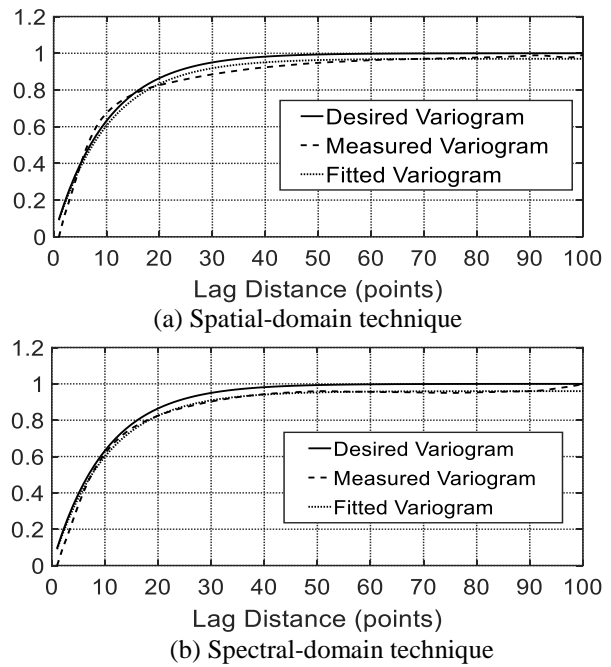


Fig. 10. Variograms of the spatially correlated rough surfaces generated by the proposed SGF correlation method and the spectral-domain method.

**B.2.1. Improved computational time**

The computational time required to generate a square random surface of  $N \times N$  points (using a specific computer) is plotted against  $N$  as shown in Fig. 11 for both the spectral-domain and the spatial-domain methods. It is clear that the spatial-domain method takes substantially less time than that taken by the spectral domain method.

Figure 12 shows a plot of the percentage of the computational time taken by the proposed spatial-domain method relative to that taken by the spectral-domain method. It is clear that the computational time is reduced by about 20%-35% when compared to the time

taken by the spectral domain method depending on the surface resolution.

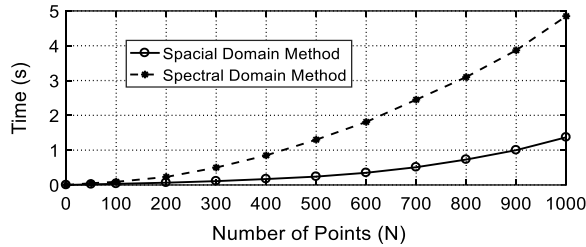


Fig. 11. Computational time required for generating square rough surface of dimensions  $N \times N$  points.

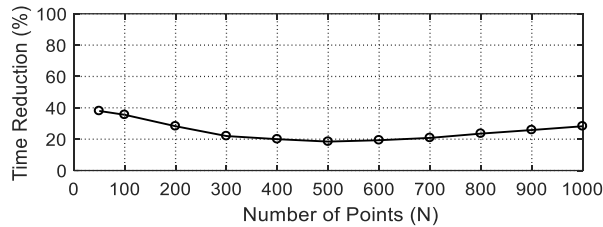


Fig. 12. Percentage of computational time taken by the proposed spatial domain method relative to that taken by the spectral domain method.

## B.2. Improved memory space

According to the algorithm of the spectral-domain method as described in Appendix A, the two-dimensional complex arrays  $F(k_p, k_q)$  and its inverse Fourier transform  $f(x_m, y_n)$  require a storage capacity of  $2 \times (N \times N) \times 16$  bytes. According to the algorithm of the spatial-domain method as described in Section VI, the two-dimensional array  $G$  requires a storage capacity of  $(N \times N) \times 8$  bytes. This means that the percentage of the memory space reduction due to the application of the spatial domain method instead of the spectral domain method can be expressed as:

$$\begin{aligned} \text{Memory Space Reduction (\%)} \\ = \frac{(N \times N) \times 8}{2 \times (N \times N) \times 16} \times 100 \% = 25 \%. \end{aligned} \quad (22)$$

## C. Polarization characteristics of the near field scattered from finite rough surfaces

The aim of this section is to find the relation between the polarization characteristics of the near field scattered from a rough surface and the geometrical and statistical properties of the surface. For this purpose, and before going into a deep study of the rough surface response to EM waves, we study the polarization characteristics of the near field scattered from a square conducting sheet whose heights are given as sinusoidal variation in one direction ( $x$ ) and constant with the other direction ( $y$ ). For polarimetry, a crossed-dipole antenna arrangement is used for transmission and reception. For accurate polarimetry, both of the crossed dipoles should

be designed to have perfectly matched impedance.

### C.1. Crossed-dipole antenna characteristics

This section is concerned with the design of the crossed-dipole antenna arrangement to get perfect impedance matching for accurate estimation of the EM polarization properties of the field scattered from the surface under consideration. This antenna arrangement consists of co-planar vertical and horizontal dipoles as shown in Fig. 13. Each dipole has a length  $l$ , diameter  $d$  and excitation gap width  $g$ . The main goal is to get the optimum values of  $l$ ,  $d$  and  $g$  for minimum return loss at the dipole antenna ports.

The dipole parameters are set to  $l = 2.7 \text{ cm}$ ,  $d = l/20$  and  $g = l/18$ . The numerical results for the variation of the input impedance of this dipole with the frequency are presented in Fig. 14. It is shown that the imaginary part of the input impedance is zero at a frequency of 4343 MHz where the real part is about  $44 \Omega$ . To obtain perfect matching of the dipole antenna the operation should be achieved at this frequency with  $Z_0$  set to  $44 \Omega$  in the numerical simulation. Figure 14 shows a plot of the reflection coefficient,  $S_{11}$ , against the frequency. It is shown that  $S_{11}$  has a minimum value of  $-47 \text{ dB}$  at a frequency of 4343 MHz.

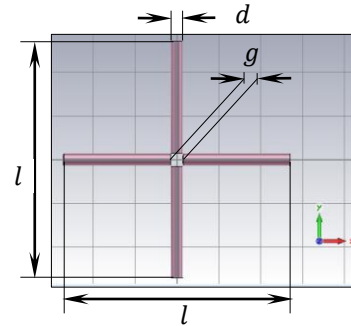


Fig. 13. The crossed-dipole antenna arrangement.

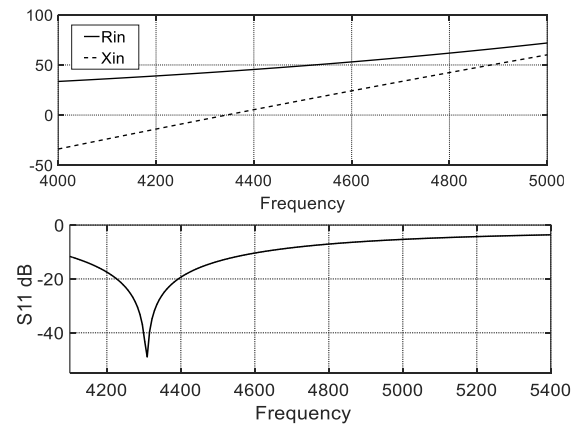


Fig. 14. Variation of the dipole input impedance and the reflection coefficient  $S_{11}$  with the frequency;  $l = 2.7 \text{ cm}$ ,  $d = l/20$  and  $g = l/18$ .

## C.2. Mutual coupling between sinusoidal surface and a nearby antenna

A surface taking the shape of sinusoidal wave is generated with a wave length of  $\lambda_s$  and is placed in the  $xy$  plane. The heights of the points of this surface are described by the equation,

$$z(x) = A \sin\left(\frac{2\pi x}{\lambda_s}\right), \quad (22)$$

where  $A$  is the amplitude of the sinusoidal height variations. The surface dimensions are set to  $20 \times 20$  cm,  $A = 0.8$  cm and  $\lambda_s = 1.7$  cm.

As shown in Fig. 15, the crossed dipole antennas described in section V are located at a distance  $L_x = 1.72$  cm from the sinusoidal sheet. The plane of the crossed dipoles is parallel to the sheet. The scattering parameters required to study the polarization characteristics of the near field are calculated as described in section V. For convenience, the  $y$ -oriented dipole will be referred to as the vertical dipole whereas the  $x$ -oriented dipole will be referred to as the horizontal one. For demonstrating the dependence of the backscattered field on the orientation of the sinusoidal sheet the scattering parameters are calculated while the surface rotates from  $0^\circ$  to  $90^\circ$  about the  $z$ -axis.

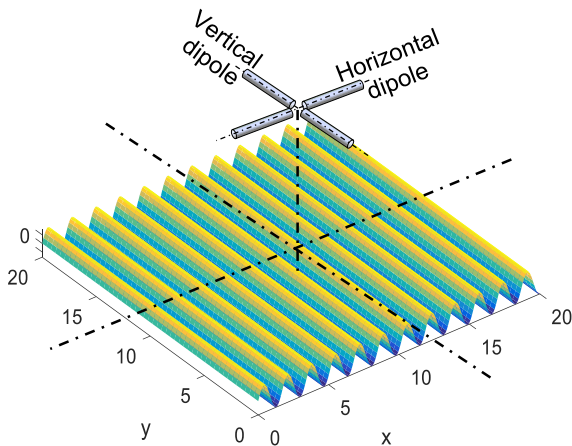


Fig. 15. The crossed dipole antennas are placed facing the center of the sinusoidal sheet.

The co-polarized scattering parameters  $S_{11}$  and  $S_{22}$  and the cross-polarized scattering parameters  $S_{12}$  and  $S_{21}$  are plotted with the angle of rotation ( $\theta$ ) of the sinusoidal sheet. As shown in Fig. 16, the scattering parameter of the vertical dipole  $S_{11}$  has a value of  $-7.4$  dB at  $\theta = 0^\circ$  where the vertical dipole is parallel to the straight lines of the sinusoidal sheet. With increasing the angle of rotation, the scattering parameter  $S_{11}$  decreases reaching a minimum value of  $-11$  dB at  $\theta = 90^\circ$  where this dipole is perpendicular to the straight lines of the sinusoidal sheet. Similarly, the scattering parameter  $S_{22}$  reaches a maximum value of  $-7.2$  dB at  $\theta = 90^\circ$  and a minimum value of  $-11$  dB at  $\theta = 0^\circ$ .

As shown in Fig. 16, the cross-polarized parameters  $S_{12}$  and  $S_{21}$  have their minimum values ( $-69.8$  dB) at  $\theta = 0^\circ$  and  $\theta = 90^\circ$ , i.e., when one of the dipoles is parallel to the straight lines of the sinusoidal sheet. They reach their maximum values ( $-15$  dB) at  $\theta = 45^\circ$ , i.e., when the straight lines of the sinusoidal sheet make an angle of  $45^\circ$  with each dipole.

In conclusion, the orientation of the sinusoidal sheet around the  $z$ -axis can be indicated by the scattering parameters  $S_{11}$ ,  $S_{22}$ ,  $S_{21}$  and  $S_{12}$ , and hence these scattering parameters can be used as polarimetric parameters for scatterers having geometrical shape similar to the sinusoidal sheet.

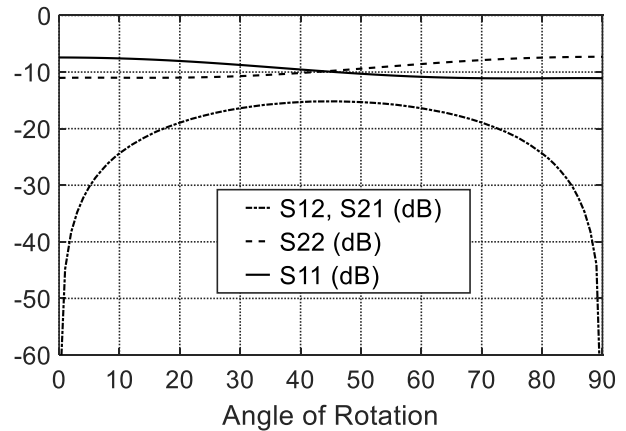


Fig. 16. Variation of the scattering parameters ( $S_{11}$ ,  $S_{22}$ ,  $S_{21}$  and  $S_{12}$ ) with the rotational angle of the sinusoidal surface around  $z$ -axis.

## C.3. Ensemble size for converging backscattering coefficients

The purpose of the following discussion is to investigate the rate of convergence of the coefficients of backscattering from rough surfaces generated using both the spectral-domain and the spatial-domain methods with increasing the ensemble size (number of sample rough surfaces over which the results are averaged). More precisely, it is required to get the minimum size of the ensemble to get converging results.

For this purpose, a crossed-dipole antenna with same parameters as described in Section VI.C.1 is placed at a distance  $L = 1.72$  cm from a  $20 \times 20$  cm rough surface of the statistical parameters:  $l_{cx} = l_{cy} = 1.8$  cm,  $h_{rms} = 0.5$  cm. The scattering parameters  $S_{11}$  and  $S_{22}$  representing copolarized backscattered EM field are investigated at  $f = 4343$  MHz.

The results for the variation of the averaged  $S_{11}$  and  $S_{22}$  with the ensemble size using the spectral and spatial domain methods are presented in Fig. 17 and Fig. 18, respectively. It is clear that both methods are fast convergent and a minimum ensemble size of 5 is fairly acceptable for both of them.

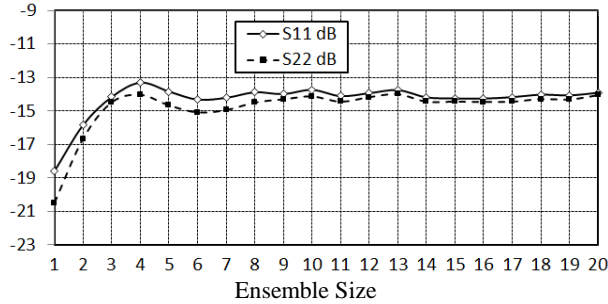


Fig. 17. Convergence of  $S_{11}$  and  $S_{22}$  with increasing the ensemble size of rough surfaces generated using the spectral domain method.

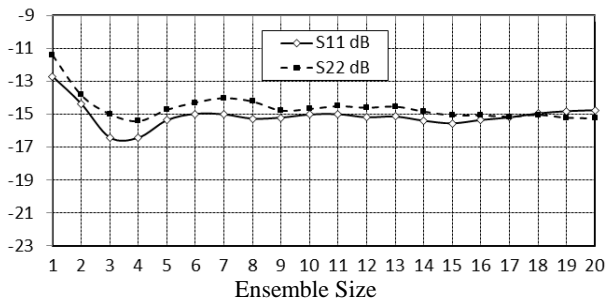


Fig. 18. Convergence of  $S_{11}$  and  $S_{22}$  with increasing the ensemble size of rough surfaces generated using the spatial domain method.

#### C.4. Polarization characteristics of the mutual coupling between rough surfaces and nearby antennas

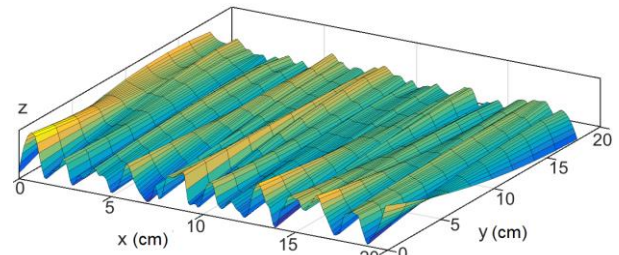
In this section we study the EM scattering from various anisotropic rough surfaces; each with a correlation length in one direction relatively larger than that in the perpendicular direction, for example,  $l_{cy} > l_{cx}$ . It is expected that the larger the ratio  $l_{cy}/l_{cx}$ , the closer the polarization characteristics of the near field scattered from the rough surface to that of the sinusoidal sheet studied in Section VI.C.2.

For this purpose, we demonstrate anisotropic rough surfaces with various ratios of the correlation lengths:  $l_{cy}/l_{cx} = 20, 10, 5, 1$ ; each with dimensions  $20 \times 20$  cm. The geometrical models of these rough surfaces are presented in Fig. 19. The scattering parameters concerning the co-polarization and cross polarization of the backscattered field are compared to those obtained for the sinusoidal surface, which are presented in Section VI.C.2.

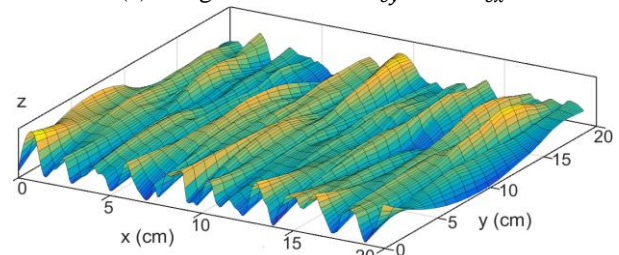
Figure 20 shows the variation of the co-polarized and cross-polarized scattering parameters with the rotational angle  $\theta$ , from  $\theta = 0^\circ$  to  $\theta = 90^\circ$  for each of the rough surfaces described above.

In Fig. 20 (a) it is clear that, for the rough surface with  $l_{cy}/l_{cx} = 20$ , the variations of both the co-polarized and cross-polarized scattering parameters with

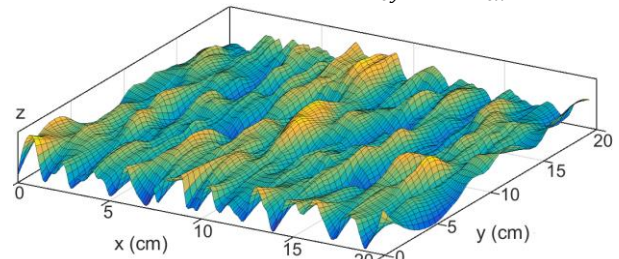
the rotational angle  $\theta$  are closer to the behavior of those parameters for the sinusoidal sheet presented in Fig. 16. The maximum difference between  $S_{11}$  and  $S_{22}$  occurs at  $\theta = 0^\circ$  and  $\theta = 90^\circ$  where it is equal to about  $\pm 2.5$  dB.



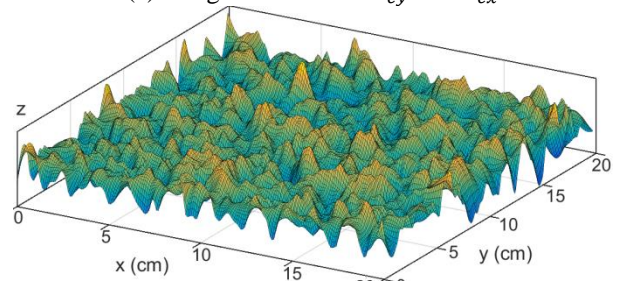
(a) Rough surface with  $l_{cy} = 20 l_{cx}$



(b) Rough surface with  $l_{cy} = 10 l_{cx}$



(c) Rough surface with  $l_{cy} = 5 l_{cx}$



(d) Rough surface with  $l_{cy} = l_{cx}$

Fig. 19. The generated rough surfaces with different correlation lengths.

For such a rough surface, the cross-polarized scattering parameters  $S_{12}$  and  $S_{21}$  have their minimum values (about  $-40$  dB) near  $\theta = 0^\circ$  and  $\theta = 90^\circ$ , i.e., when one of the dipoles is approximately parallel to the direction of the larger correlation length. They reach their maximum values (about  $-23$  dB) near  $\theta = 45^\circ$ , i.e., when each dipole makes an angle of about  $45^\circ$  with the direction of larger correlation length. This makes

analogy with the same results concerning the sinusoidal sheet, presented in Fig. 16.

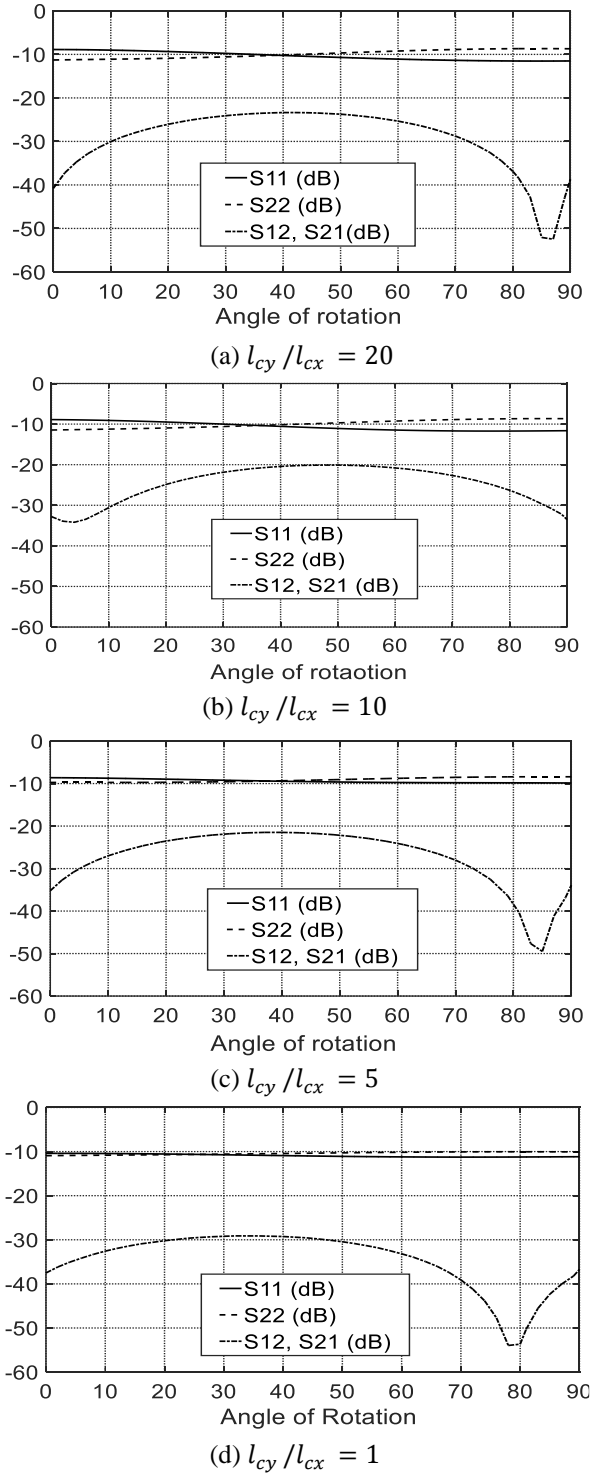


Fig. 20. Variation of the scattering parameters with the rotational angle of the rough surface around  $z$  considering the backscattered field from a  $20 \times 20$  cm rough surface of  $l_{cx} = 0.85$  cm,  $h_{rms} = 0.4$  cm.

For the rough surfaces with lower ratios ( $l_{cy}/l_{cx}$ ), the behaviour of both the co-polarized and cross-polarized scattering parameters with varying the rotational angle  $\theta$  are significantly different from those of the sinusoidal sheet. For isotropic rough surface ( $l_{cy} = l_{cx}$ ), as shown in Fig. 20 (d), the parameters  $S_{11}$  and  $S_{22}$  are very close to each other indicating very weak polarization discrimination of the EM backscattering from such a surface.

## VII. SUMMARY AND CONCLUSION

A computationally efficient and inexpensive spatial-domain technique for generating spatially-correlated random rough surface with predetermined statistical properties using the SGF is described and examined by generating a variety of random rough surfaces with various statistical properties. It is shown that the generated rough surfaces fit the required Gaussian distribution and the other statistical properties including the mean value, the root-mean-squared height and the correlation lengths in the different directions with accuracy not less than 97%.

The importance of generating such rough surfaces for simulating the fully polarimetric land imaging systems are demonstrated by investigating the polarization properties of the near field scattered by various isotropic and anisotropic rough surfaces.

It is shown that the cross-polarized component of the near field scattered from anisotropic rough surfaces is significantly increased especially when the correlation length in one direction along the rough surface is much larger than that in the perpendicular direction.

For a rough surface with  $l_{cy} \gg l_{cx}$ , the cross-polarized component of the backscattered field has its minimum value near  $\theta = 0^\circ$  and  $\theta = 90^\circ$ , i.e., when one of the dipoles is approximately parallel to the direction of the larger correlation length. They reach their maximum values near  $\theta = 45^\circ$ , i.e., when each dipole makes an angle of about  $45^\circ$  with the direction of larger correlation length.

## APPENDIX A. SPECTRAL-DOMAIN METHOD OF ROUGH SURFACE GENERATION

To generate a random rough surface of dimensions  $L \times L$  with resolution  $N \times N$  discrete segments, the spectral-domain-method obtains the surface heights  $z_{mn} = f(x_m, y_n)$  by calculating the following IDFT for each point  $(x_m, y_n)$ ;  $m, n = 1, 2, \dots, N$  of a uniform horizontal two-dimensional grid [22]:

$$f(x_m, y_n) = \frac{1}{L^2} \sum_{p=-\frac{N}{2}}^{\frac{N}{2}-1} \sum_{q=-\frac{N}{2}}^{\frac{N}{2}-1} F(k_p, k_q) e^{j(k_p x + k_q y)}, \quad (\text{A.1})$$

where,

$$F(k_p, k_q) = 2\pi L \sqrt{W(k_p, k_q)} \begin{cases} \frac{N(0,1) + jN(0,1)}{\sqrt{2}}, & p, q \neq 0, \frac{N}{2} \\ N(0,1), & p, q = 0, \frac{N}{2} \end{cases} \quad (\text{A.2})$$

where  $k_p$  and  $k_q$  are the discrete set of spatial frequencies and are expressed as:

$$k_p = \frac{2\pi p}{L}, \quad k_q = \frac{2\pi q}{L}, \quad (\text{A.3})$$

$W(k_p, k_q)$  is the power spectral density function of the surface and is expressed as:

$$W(k_p, k_q) = \frac{l_{cx} l_{cy} h_{rms}}{4\pi} e^{\frac{1}{4}(-k_p^2 l_{cx}^2 - k_q^2 l_{cy}^2)}. \quad (\text{A.4})$$

For  $f(x, y)$  to be real the following condition should be satisfied:

$$F(k_p, k_q) = F^*(-k_p, -k_q). \quad (\text{A.5})$$

## REFERENCES

- [1] M. Sugimoto, K. Ouchi, and Y. Nakamura, "Four-component scattering power decomposition algorithm with rotation of covariance matrix using ALOS-PALSAR polarimetric data," *Remote Sensing*, vol. 4, no. 8, pp. 2199-2209, July 2012.
- [2] A. Nascimento, A. Frery, and R. Cintra, "Detecting changes in fully polarimetric SAR imagery with statistical information theory," *IEEE Transactions on Geoscience and Remote Sensing*, vol. 4, Sep. 2018.
- [3] W. Wang, et al., "A fully polarimetric SAR imagery classification scheme for mud and sand Flats in intertidal zones," *IEEE Transactions on Geoscience and Remote Sensing*, vol. 55, no. 3, pp. 1734-1742, Mar. 2017.
- [4] Y. Zhang, Yu Li, X. San Liang, and J. Tsou "Comparison of oil spill classifications using fully and compact polarimetric SAR images," *Applied Sciences*, vol 7, no. 2, pp. 193-214, Feb. 2017.
- [5] S. Uhlmann and S. Kiranyaz "Integrating color features in polarimetric SAR Image classification," *IEEE Transactions on Geoscience and Remote Sensing*, vol. 52, no. 4, pp. 2197-2216, Apr. 2014.
- [6] L. Zhang, L. Sun, B. Zou, and W. Moon, "Fully polarimetric SAR image classification via sparse representation and polarimetric features," *IEEE Journal of Selected Topics in Applied Earth Observations and Remote Sensing*, vol. 8, no. 8, pp. 3923-3932, Aug. 2015.
- [7] B. Zhang, W. Perrie, Paris W. Vachon, X. Li, W. Pichel, J. Guo, and Y. He, "Ocean vector winds retrieval from C-band fully polarimetric SAR measurements," *IEEE Transactions on Geoscience and Remote Sensing*, vol. 50, no. 11, pp. 4252-4261, Nov. 2012.
- [8] C. Hsieh, "Energy transition for depolarized backscatter from rough surfaces," *Journal of Microwave Power and Electromagnetic Energy*, vol. 44, no. 3, pp. 132-138, Jan. 2010.
- [9] N. Sajjad, A. Khenchaf, and A. Coatanhay, "Depolarization of electromagnetic waves from sea surface," *In OCOSS. European Conf.*, June 2010.
- [10] A. Sentenac, H. Giovannini, and M. Saillard, "Scattering from rough inhomogeneous media: Splitting of surface and volume scattering," *JOSA A*, vol. 19, no. 4, pp. 727-736, Apr. 2002.
- [11] K. O'Donnell and E. Mendez, "Experimental study of scattering from characterized random surfaces," *JOSA A*, vol. 4, no. 7, pp. 1194-1205, July 1987.
- [12] M. Zubair, Z. Haider, S. Khan, and J. Nasir, "Atmospheric influences on satellite communications," *Przeglad Elektrotechniczny*, vol. 87, no. 5, pp. 261-264, Jan. 2011.
- [13] G. Wolosinski, V. Fusco, and P. Rulikowski, "Broadband dual-polarized antenna with high port isolation and polarization purity," *In Antennas and Propagation (APSURSI), IEEE International Symposium on*, pp. 1581-1582, June 2016.
- [14] C. Holler, A. Taylor, M. Jones, O. King, S. Muchovej, M. Stevenson, R. Wylde, et al., "A circularly symmetric antenna design with high polarization purity and low spillover," *IEEE Transactions on Antennas and Propagation*, vol. 61, no. 1, pp. 117-124, Jan. 2013.
- [15] J. M. Ralston and E. L. Ayers, "Antenna effects on polarimetric imagery in ultrawide synthetic aperture radar," *Institute for Defense Analyses*, No. IDA-D-2735, Alexandria, Virginia Sep. 2002.
- [16] Y. Cocheri and R. Vauzelle, "A new ray-tracing based wave propagation model including rough surfaces scattering," *Progress In Electromagnetics Research*, vol. 75, pp. 357-381, 2007.
- [17] S. Coons, "Surfaces for computer aided design of space forms," *Massachusetts Inst. of Tech. Cambridge Project Mac*, no. MAC-TR-41, June 1967.
- [18] M. Escobar and A. Meyerovich, "Applications and identification of surface correlations," *arXiv Preprint arXiv:1404.1291*, vol. 2, Apr. 2014.
- [19] C. Mack, "Generating random rough edges, surfaces and volumes," *Applied Optics*, vol. 52, no. 7, pp.1472-1480, 1 Mar. 2013.
- [20] A. Francisco and N. Brunetière, "A hybrid method for fast and efficient rough surface generation," *Proceedings of the Institution of Mechanical Engineers*, vol. 230, no. 7, pp. 747-768, July 2016.
- [21] K. Uchida, J. Honda, and K. Y. Yoon, "An algorithm for rough surface generation with inhomogeneous parameters," *Journal of Algorithms & Computational Technology*, vol. 5, no. 2, pp.

- 259-271, June 2011.
- [22] Y. Kuga and P. Phu, "Experimental studies of millimeter - wave scattering in discrete random media and from rough surfaces," *Progress In Electromagnetics Research*, vol. 14, no. 7, pp. 37-88, 1996.
- [23] K. Uchida, M. Takematsu, and J. Honda, "A discretization criterion for generating random rough surface based on convolution method," *Complex, Intelligent and Software Intensive Systems (CISIS), Eighth International Conference, IEEE*, pp. 307-312, July 2014.
- [24] T. Jacobs, et al., "Quantitative characterization of surface topography using spectral analysis," *Surface Topography: Metrology and Properties*, Vol. 5, no. 1 p. 013001, Jan. 2017.
- [25] S. Abraham and M. Golay, "Smoothing and differentiation of data by simplified least squares procedures," *Analytical Chemistry*, vol. 36 no. 8, pp. 1627-1639, July 1964.
- [26] R. Torala and A. Chakrabarti, "Generation of Gaussian distributed random numbers by using a numerical inversion method," *Computer Physics Communications*, vol. 74, no. 3, pp. 327-334, Mar. 1993.
- [27] D. Thomas, W. Luk, P. Leong, and J. Villasenor, "Gaussian random number generators," *ACM Computing Surveys*, vol. 39, no. 4, p. 11, Nov. 2007.
- [28] R. Ritabrata, "Comparison of Different Techniques to Generate Normal Random Variables," *Stochastic Signals and Systems (ECE 330: 541)*, Rutgers, The State University of New Jersey, Nov. 2002.